The transcriptional repressor orphan nuclear receptor TLX is responsive to caffeine and istradefylline

Giuseppe Faudone[a], Whitney Kilu[a], Xiaomin Ni[a,b], Apirat Chaikuad[a,b], Sridhar Sreeramulu[c], Pascal Heitel[a], Harald Schwalbe[c], Stefan Knapp[a,b], Manfred Schubert-Zsilavecz[a], Jan Heering[d], and Daniel Merk[a]*

[a] Institute of Pharmaceutical Chemistry, Goethe University Frankfurt, Max-von-Laue-Str. 9, D-60438 Frankfurt, Germany

[b] Structural Genomics Consortium, BMLS, Goethe University Frankfurt, Max-von-Laue-Str. 15, D-60438 Frankfurt, Germany

[c] Center for Biomolecular Magnetic Resonance (BMRZ), Institute for Organic Chemistry and Chemical Biology, Goethe University Frankfurt, Max-von-Laue-Str. 7, D-60438 Frankfurt, Germany

[d] Fraunhofer Institute for Translational Medicine and Pharmacology ITMP, Theodor-Stern-Kai 7, D-60596 Frankfurt, Germany

* Correspondence to: merk@pharmchem.uni-frankfurt.de

Abstract. The orphan nuclear receptor TLX is expressed almost exclusively in neural stem cells. TLX acts as an essential factor for neural stem cell survival and is hence considered as a promising drug target in neurodegeneration. However, few studies have characterized the roles of TLX due to a lack of ligands and limited functional understanding. Here, we identify caffeine and istradefylline as TLX ligands that counteract the receptor's intrinsic repressor activity in reporter gene assays and modulate TLX regulated SIRT1 and p21 expression. Mutagenesis of residues lining a cavity within the TLX ligand binding domain altered activity of these ligands suggesting direct interactions with helix 5. Using istradefylline as a tool compound, we observed ligand-sensitive recruitment of the co-repressor SMRT and heterodimerization of TLX with RXR. Both protein-protein complexes evolve as factors that modulate TLX function and suggest an unprecedented role of TLX in directly repressing other nuclear receptors.

Introduction

The human homologue of drosophila tailless gene tll, TLX (NR2E1), is a member of the nuclear receptor (NR) family which act as ligand-dependent transcriptional regulators. In adults, expression of TLX is strongly limited to adult neural stem cells (NSCs) residing in the subventricular zone and dentate gyrus of the hippocampus as well as in retinal progenitor cells[1,2]. According to rodent models, TLX is required to maintain NSCs in an undifferentiated proliferating state and its mutations cause disruption of neurogenesis in NSCs[3]. In mice and drosophila, TLX knockout results in severe aggressiveness, abnormal brain development and retinal dystrophies[4,5]. Moreover, TLX appears to play a crucial role in spatial learning and cognitive functions during adolescence and adulthood[6–8]. Therefore, dysregulation of TLX has been associated with mental illness including bipolar disorders and schizophrenia[9]. Beyond these roles in neurological homeostasis and brain function, recent reports have suggested a potential tumorigenic activity of the orphan NR due to marked overexpression in glioblastoma and neuroblastoma cell lines[10,11]. These lines of evidence suggest TLX as an attractive target for neurodegenerative diseases and malignant brain tumors.

Endogenous TLX ligands, forming an essential part of the NR function, remain elusive and only few synthetic TLX modulators with limited potency have been described to date[12–14]. In light of its obvious therapeutic potential, further evaluation of the receptor's function and the discovery of potent TLX ligands are imperative.

Here, we identify xanthine derivatives as TLX modulators. Based on the identified caffeine (**8**, Figure 1) as a lead compound, our structure-activity relationship study succeeded in tuning the potency of this chemotype to nanomolar activities sufficient for the use as a pharmacological tool. Additionally, the structurally related and recently approved anti-Parkinson drug istradefylline emerged as a potent TLX modulator with low nanomolar potency. Mutagenesis studies defined a molecular epitope of TLX modulation by this class of TLX ligands to a region inside the ligand binding domain (LBD) involving interaction with helix 5. We observed also heterodimerization of TLX with retinoid X receptor (RXR) as well as recruitment of the nuclear receptor co-repressor 2 (SMRT). We demonstrated that istradefylline robustly displaced this repressor from TLX and modulated dimerization aligning with its effects on cellular TLX activity. This observation also suggests unprecedentedly a role of TLX as a direct repressor for other nuclear receptors. Overall, our results provide potent TLX modulators to study the receptor's role in health and disease and as a chemical starting point to facilitate future TLX ligand discovery.

Results and Discussion

As an essential basis to identify and characterize TLX ligands we established a hybrid reporter gene assay to capture TLX activity in a bidirectional fashion by combining Gal4-TLX with the potent transcriptional inducer Gal4-VP16[15] (see Supporting Information and Figure S1). This artificial system reflected the repressor activity of TLX[16–19] and simultaneously enabled potent control experiments to confirm TLX modulation. We also demonstrated that this VP16/TLX assay was representative of cellular TLX function. When we co-transfected Gal4-TLX with constitutively active NRs (Nurr1 or RORα resembling VP16 as ligand-independent transcriptional inducer) or NRs with low intrinsic activity in Gal4 format, a dose-dependent repression of reporter activity by TLX could be observed (Figure S1b&c) corroborating the VP16/TLX assay setting as suitable to discover and profile small molecule modulators of TLX activity. These cellular experiments indicated TLX-mediated effects on the activity of a variety of NRs. To confirm this observation in a cell-free setting, and to determine whether direct interactions are involved, we probed dimerization of TLX with RXR by titrating Tb^{3+}-cryptate-labeled TLX LBD with GFP-labeled RXRα LBD in a homogenous time-resolved fluorescence resonance energy transfer (HTRF) assay. We detected strong RXR-TLX heterodimerization with an EC_{50} value of 120 nM (Figure S1d) suggesting an unprecedented direct repressor activity of TLX on nuclear receptors and further validating the VP16/TLX assay setting as highly suitable to study TLX modulation by small molecules.

Using the VP16/TLX reporter gene assay, we then screened a drug fragment library comprising 480 small organic molecules (MW range 80-300 g/mol) for TLX modulatory activity and discovered 1-methylxanthine (**1**) as TLX modulator that diminished TLX-mediated transcriptional repression with an IC_{50} value of 9±3 µM (Table 1) suggesting inverse agonism. Intrigued by this activity, we studied the structurally related xanthines **2-8** for TLX modulation. **2-4** and **7** were inactive on TLX whereas theophylline (**5**), paraxanthine (**6**) and caffeine (**8**, Figure 1) counteracted TLX-dependent transcriptional repression as well. Control experiments in absence of the Gal4-TLX hybrid receptor revealed no unspecific effects of the xanthines confirming their TLX-mediated activity (Figure 1b). With caffeine (**8**) as a first TLX modulator tool compound in hand, we studied its effect on TLX repressor activity on NRs to probe its response to ligands. When Gal4-TLX and a human NR in Gal4 format were co-transfected, caffeine (**8**, 30 µM) reversed the repressor activity of TLX (Figure 1d, Figure S2). Such activity was observed for constitutively active NRs (e.g. Nurr1) and for NRs with low intrinsic activity (e.g. RARα, FXR and RXRα). Of note, caffeine (**8**) selectively modulated TLX amongst NRs (Figure S3) except a slight additive activity with the reference agonist T0901317 on LXRs further demonstrating that its effects were TLX mediated.

3

Table 1. Activity of xanthines **1**-**8** on TLX in the VP16/TLX setting. Compounds were tested to a maximum concentration of 100 µM. Fold repression refers to the maximum fold increase in reporter activity (compared to 0.1% DMSO) resulting from inhibition of TLX. Control experiments in absence of Gal4-TLX have confirmed TLX mediated effects for all actives. All data are the mean±S.E.M., n≥3.

ID	name	R^1	R^2	R^3	IC_{50} (fold TLX repression)
2	xanthine	H	H	H	inactive at 100 µM
1	1-methylxanthine	Me	H	H	9±3 µM (2.3±0.3)
3	3-methylxanthine	H	Me	H	inactive at 100 µM
4	7-methylxanthine	H	H	Me	inactive at 100 µM
5	theophylline	Me	Me	H	10±2 µM (2.6±0.1)
6	paraxanthine	Me	H	Me	11±2 µM (2.4±0.1)
7	theobromine	H	Me	Me	inactive at 100 µM
8	caffeine	Me	Me	Me	9±2 µM (2.3±0.1)
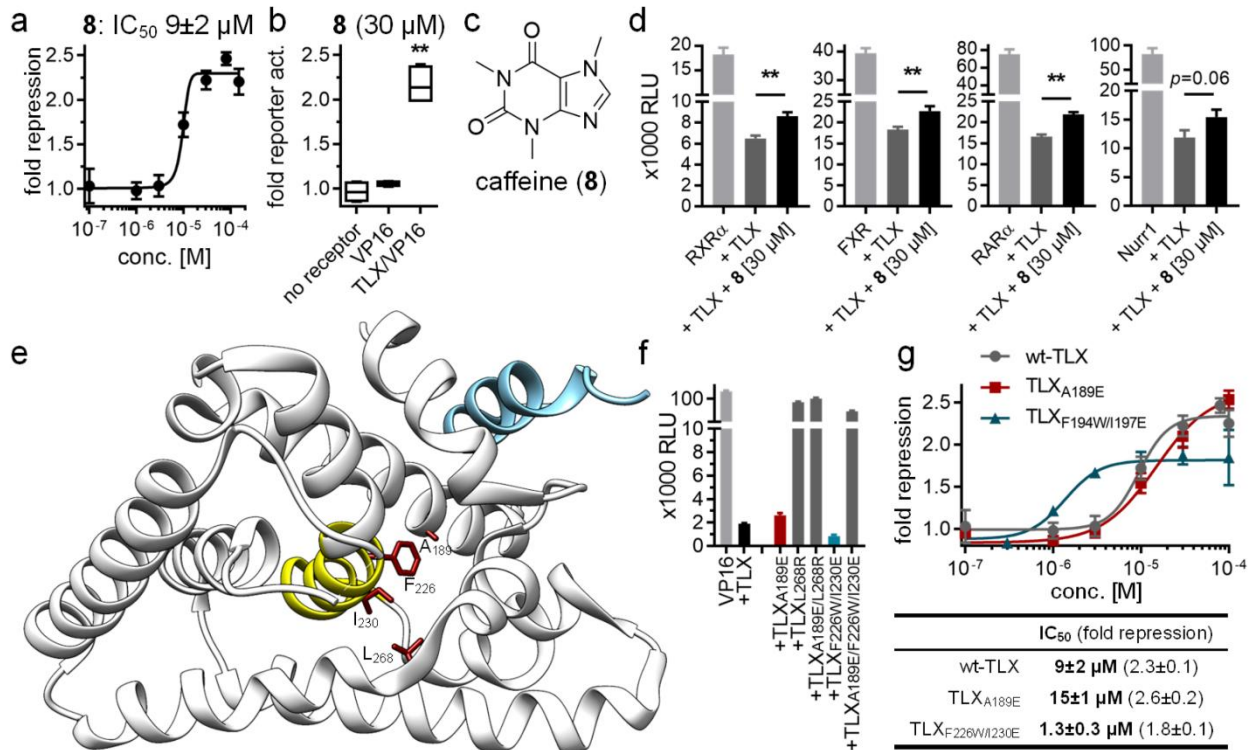
Figure 1. Caffeine (**8**) acts as a TLX ligand. (a) Dose-response curve in the VP16/TLX reporter gene assay. Data are the mean±S.E.M., n≥3. The underlying reporter and control data are shown in Figure S4. (b) Control experiments (no Gal4 hybrid receptor and Gal4-VP16 alone) confirm TLX mediated activity of **8**. Boxplots show min.-max. fold reporter activation compared to 0.1% DMSO in the respective setting. ** p < 0.01; n=4. (c) Structure of caffeine (**8**). (d) Caffeine (**8**) reverses repressor activity of TLX on NRs. Data are the mean±S.E.M., n≥3. ** p < 0.01. (e-g) Mutagenesis of TLX. (e) TLX LBD (apo, PDB-ID: 4XAJ[20]) with residues for mutagenesis in red, helix 5 in yellow and bound co-regulator in blue. (f) Activity of wt-TLX and mutants on Gal4-VP16 induced reporter activity. TLX$_{A189E}$ and TLX$_{F226W/I230E}$ are functional repressors. Data are the mean±S.E.M., n=3. (g) Dose-response curves of caffeine (**8**) on wt-TLX (grey) and the mutants TLX$_{A189E}$ (red) and TLX$_{F226W/I230E}$ (blue). F226W/I230E decreases the IC_{50} value of caffeine (**8**). Fold repression refers to the maximum fold increase in reporter activity compared to 0.1% DMSO in the respective setting. Data are the mean±S.E.M., n≥3.

In an attempt to define key residues involved in TLX modulation by caffeine (**8**) as basis for future TLX ligand discovery, we performed a preliminary mutagenesis study. From the only available TLX X-ray apo-structure 4XAJ[20] we hypothesized a potential binding region for **8** in the cavity inside the TLX LBD protein clamped between residues A189, F226, I230 and L268 (Figure 1e). We mutated these residues by site-directed mutagenesis in the Gal4-TLX construct and employed the resulting mutants in the VP16/TLX reporter gene assay setting with equal conditions as used for wt-TLX to evaluate their impact on TLX activity (Figure 1f) and TLX modulation by caffeine (Figure 1g).

TLX_{A189E} retained the repressor activity of wt-TLX while TLX_{L268R} turned out as almost inactive concerning repression of VP16-induced reporter expression (Figure 1e). Combination of both mutations for a potential intramolecular salt bridge in $TLX_{A189E/L268R}$ led to inactivity as well. Mutagenesis of F226 and I230 in $TLX_{F226W/I230E}$ produced another functional mutant while the triple mutant $TLX_{A189E/F226W/I230E}$ was only a weak transcriptional repressor and not suitable for further studies. These observations indicated that the mutations L268R, A189E/L268R and A189E/F226W/I230E compromised expression, stability or activity of apo-TLX and were not suitable for further evaluation. The activity of mutants TLX_{A189E} and $TLX_{F226W/I230E}$, in contrast, resembled wt-TLX in the VP16/TLX assay suggesting them as functional. Using the mutants TLX_{A189E} and $TLX_{F226W/I230E}$ in the VP16/TLX assay setting, we recorded dose-response curves of caffeine (**8**) to compare effects on wt-TLX and mutants (Figure 1g). While the activity of **8** was hardly altered by the A189E mutation, caffeine (**8**) revealed an almost 10-fold increased potency on $TLX_{F226W/I230E}$ suggesting that residues located in helix 5 in the core region of the LBD are involved in mediating TLX modulation by **8**.

Our observations characterize caffeine (**8**) as a direct TLX modulator exhibiting inverse agonism in the VP16/TLX assay. The natural product thus appeared attractive for structural optimization as TLX modulator. The activity data of **1**-**8** demonstrate that alkylation in 1-position is essential. We next studied the biological activity of further derivatized caffeine analogues (Table 2) focusing on the remaining free 8-position of xanthines.

The endogenous metabolite uric acid (**9**) turned out inactive on TLX while methylated uric acid derivatives **10**-**12** comprised weak activity. Similar as observed for the xanthines, uric acid derivatives also required 1-methyl substitution to exhibit TLX modulation. Substituents in 8-position of xanthines (**13**-**15**) had pronounced effects on TLX modulatory activity. 8-Bromotheophylline (**13**) displayed slightly stronger potency compared to **5** while the 8-chlorine analogue **14** was less active suggesting preference for bulky moieties in this region. The extended 8-phenyltheophylline (**15**) indeed comprised remarkably enhanced, submicromolar activity on TLX prompting us to study the potential of expanding the 8-phenyl residue with substituents (Table 3).

Table 2. Activity of **9-15** on TLX in the VP16/TLX setting. **5** and **8** for comparison. Compounds were tested to a maximum concentration of 100 µM. Fold repression refers to the maximum fold increase in reporter activity (compared to 0.1% DMSO) resulting from inhibition of TLX. Control experiments in absence of Gal4-TLX have confirmed TLX mediated effects for key compounds. All data are the mean±S.E.M., n≥3.

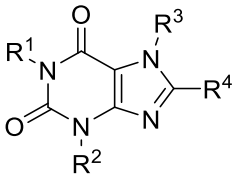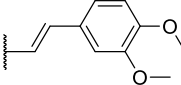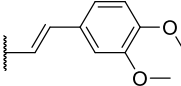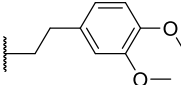| ID	R^1	R^2	R^3	X-Y	R^4	IC_{50} (fold TLX repression)
5	Me	Me	H	N=C	H	10±2 µM (2.6±0.1)
8	Me	Me	Me	N=C	H	9±2 µM (2.3±0.1)
9	H	H	H	HN-C	=O	inactive at 100 µM
10	Me	H	H	HN-C	=O	25±3 µM (1.7±0.1)
11	Me	H	Me	HN-C	=O	44±4 µM (3.0±0.2)
12	Me	Me	Me	HN-C	=O	24±3 µM (2.7±0.2)
13	Me	Me	H	N=C	Br	6±3 µM (1.6±0.1)
14	Me	Me	H	N=C	Cl	17±3 µM (2.1±0.2)
15	Me	Me	H	N=C	Ph	0.5±0.3 µM (2.4±0.2)

Synthesis of analogues **16-29**, **31-34** was accomplished by Suzuki coupling of 8-bromotheophylline with arylboronic acids or by cyclization of the respective 5,6-diamino-1,3-dialkylpyrimidine-2,4(1*H*,3*H*)-dione with arylcarboxylates (Supporting Information). We prepared all tolyl (**16-18**), chlorophenyl (**19-21**), methoxyphenyl (**22-24**) and biphenyl (**25-27**) regioisomers of **15** from which the activity data indicated a common preference for derivatizations of **15** in *meta*-position (**17**, **20**, **23**). The chlorine substituent (**19-21**) was generally less favored in terms of efficacy and the bulkier biphenyl analogues (**25-27**) exhibited lower potency. *Meta*-methoxy analogue **23** possessed the most favorable profile regarding potency and efficacy. We hypothesized that this might be mimicked by furan analogues which simultaneously would promote solubility, and thus characterized the furan derivatives **28** and **29** of which the 3-furyl isomer **29** exhibited further enhanced activity on TLX. **29** emerged as the most active xanthine derivative with an IC_{50} value of 160 nM corresponding to approx. 50-fold higher potency compared to caffeine (**8**).

The recently approved adenosine A2 (A_{2A}) receptor antagonist istradefylline (**30**) shares the 8-substituted xanthine scaffold of this TLX ligand chemotype, prompting us to evaluate a potential interaction of **30** with TLX. Dose-response characterization of **30** in the VP16/TLX assay setting indeed demonstrated inverse TLX agonism with an IC_{50} value of 40 nM and 2.6-fold max. repression of TLX activity. Transferring the 3,4-dimethoxystyryl moiety of **30** to the theophylline scaffold in **31** resulted in a strong TLX modulator with enhanced efficacy but with reduced potency compared to **30** suggesting that the bulkier 1- and 3-substituents in istradefylline (**30**) contributed

to its potency on TLX. Reduction of the styryl residue in **31** to a phenethyl substituent in **32** retained high efficacy but was not favored in terms of IC_{50} value.

Table 3. Activity of **15**-**34** on TLX in the VP16/TLX setting. Compounds were tested to a maximum concentration of 30 µM. Fold repression refers to the maximum fold increase in reporter activity (compared to 0.1% DMSO) resulting from inhibition of TLX. Control experiments in absence of Gal4-TLX have confirmed TLX mediated effects for key compounds. All data are the mean±S.E.M., n≥3.

ID	R^1	R^2	R^3	R^4	IC_{50} (fold TLX repression)
15	Me	Me	H	Ph	0.5±0.3 µM (2.4±0.2)
16	Me	Me	H	2-CH_3-Ph	0.7±0.2 µM (2.9±0.1)
17	Me	Me	H	3-CH_3-Ph	0.5±0.2 µM (2.5±0.1)
18	Me	Me	H	4-CH_3-Ph	7±4 µM (5.0±0.7)
19	Me	Me	H	2-Cl-Ph	0.5±0.3 µM (2.1±0.2)
20	Me	Me	H	3-Cl-Ph	0.23±0.08 µM (2.4±0.1)
21	Me	Me	H	4-Cl-Ph	0.34±0.07 µM (2.1±0.1)
22	Me	Me	H	2-CH_3O-Ph	< 1.5 fold repression
23	Me	Me	H	3-CH_3O-Ph	0.3±0.1 µM (2.7±0.1)
24	Me	Me	H	4-CH_3O-Ph	4±2 µM (3.6±0.2)
25	Me	Me	H	2-biphenyl	1.8±0.6 µM (2.4±0.2)
26	Me	Me	H	3-biphenyl	< 1.5 fold repression
27	Me	Me	H	4-biphenyl	7±4 µM (1.7±0.1)
28	Me	Me	H	2-furyl	0.2±0.1 µM (3.0±0.1)
29	Me	Me	H	3-furyl	0.16±0.02 µM (2.9±0.1)
30	Et	Et	Me	(styryl-dimethoxyphenyl)	0.04±0.01 µM (2.6±0.2)
31	Me	Me	H	(styryl-dimethoxyphenyl)	0.19±0.06 µM (3.3±0.1)
32	Me	Me	H	(phenethyl-dimethoxyphenyl)	1.2±0.3 µM (2.5±0.2)
33	Et	Et	H	3-furyl	0.04±0.02 µM (4.0±0.3)
34	nPr	nPr	H	3-furyl	0.009±0.002 µM (3.0±0.2)

Eventually, we combined the 1,3-diethyl substitution pattern of the most active TLX ligand **30** with the favored 8-(furan-3-yl)theophylline motif (**29**) in compound **33** which exhibited equal potency and slightly higher efficacy compared to **30**. Further extension of the alkyl substituents to 1,3-dipropyl in **34** enhanced potency but was accompanied by a loss in efficacy. In summary, our preliminary optimization of the xanthine scaffold for TLX modulation succeeded by modification in 8-position and by altering the alkylation pattern. In 8-position, small heterocyclic residues were favored with the 3-furyl substituent as preferred motif and potency tended to increase with larger alkyl substituents in 1- and 3-positions.
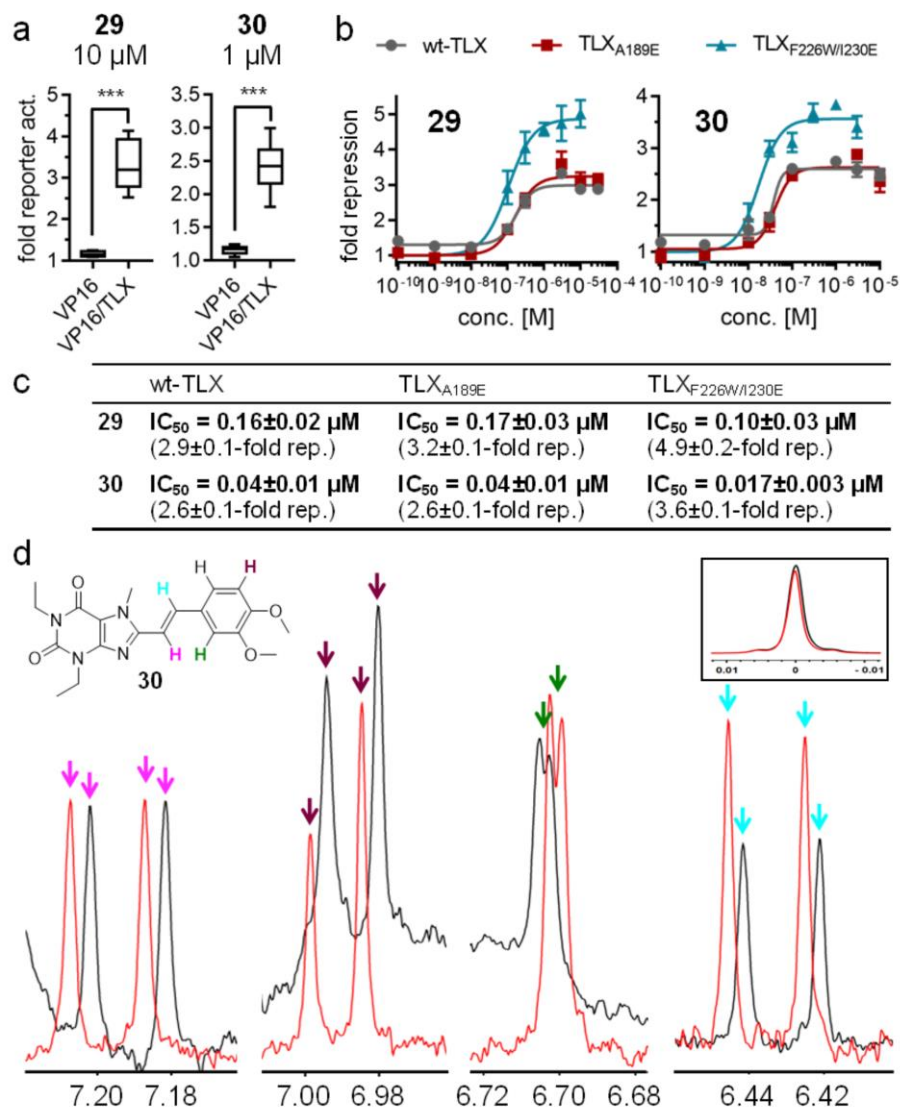
Figure 2. Interaction of **29** and **30** with TLX. (a) Control experiments involving Gal4-VP16 or Gal4-VP16 and Gal4-TLX demonstrate TLX mediated activity of **29** and **30**. Boxplots show reporter activity after treatment with **29** or **30** relative to 0.1% DMSO in the respective setting (center line, median; box limits, upper and lower quartiles; whiskers, min/max); n=6; *** p<0.001 (two-sided t-test). (b, c) TLX modulators **29** and **30** exhibited enhanced activity on TLX$_{F226W/I230E}$ mutant. (d) NMR of **30** in presence (black) or absence (red) of recombinant TLX-LBD confirms direct binding. Spectra are referenced to TMSP-Na (box). Interaction studies were performed at a ratio of 1:1 with respect to TLX and the ligand. The final [protein]-ligand concentration was 50 µM.

29 and the marketed drug **30** provided a favorable TLX modulatory profile with high efficacy and low nanomolar IC$_{50}$ values in the hybrid assay. Cellular control experiments on Gal4-VP16 confirmed TLX mediated activity of **29** and the approved drug **30** (Figure 2a) and binding to the recombinant TLX LBD was confirmed by NMR spectroscopy (Figure 2d, Figure S5). In accordance with our observation for caffeine (**8**), **29** and **30** also exhibited enhanced potency on the TLX$_{F226W/I230E}$ mutant (Figure 2b&c) suggesting that the xanthines modulate TLX via a common mechanism involving residues in helix 5 of the TLX LBD. Moreover, the TLX modulators **29** and

30 turned out inactive on RARα, PPARα, PPARγ, PPARδ, LXRα, LXRβ, FXR, VDR, CAR, RXRα, RORα, Nurr1, Nur77 and NOR1 (Figure S3) demonstrating high selectivity for TLX within the NR family.
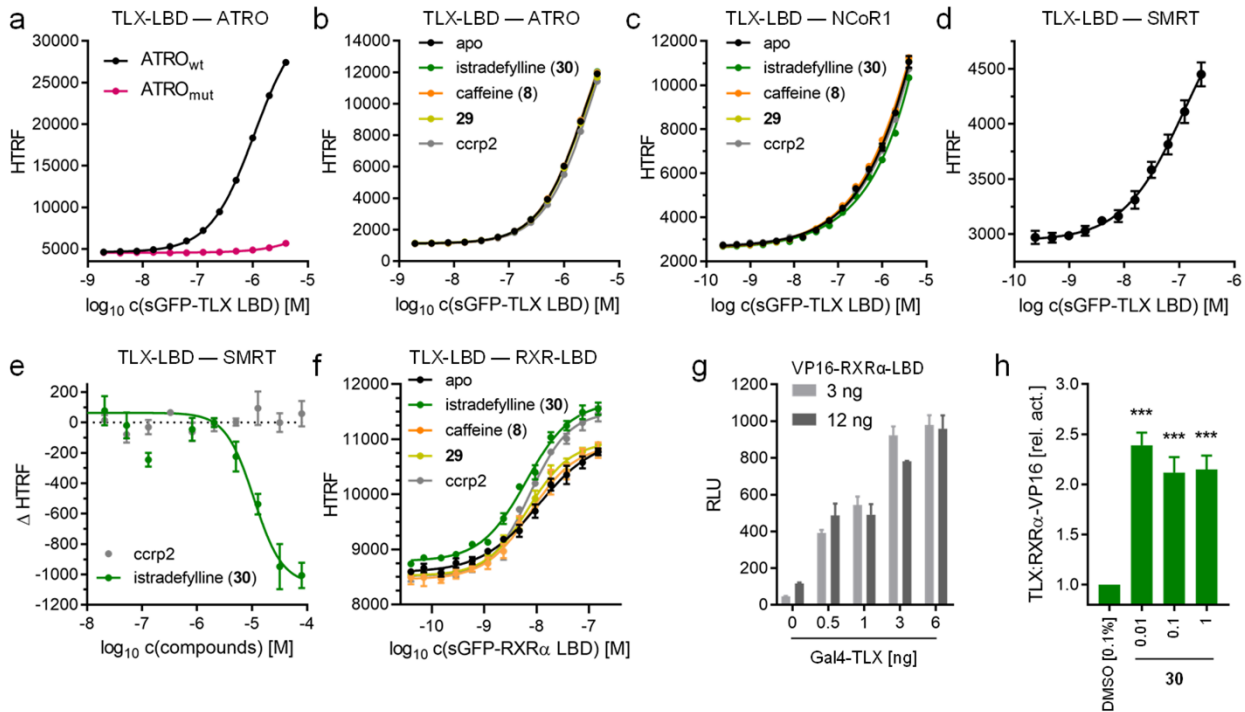
Figure 3. Co-regulator recruitment and dimerization of TLX. (a) TLX specifically interacts with the Atro box sequence[20], an interaction incompetent mutant[21] was not bound. Data are the mean±SD; N=3. (b) TLX-atrobox affinity was not modulated by **8**, **29**, **30** or the reference ligand ccrp2. All compounds were used at 10 μM. Data are the mean±SD; N=3. (c) Titration of NCoR1 with TLX confirmed a TLX-NCoR1 interaction but addition of TLX ligands had no effect. All compounds were used at 10 μM. Data are the mean±SD; N=3. (d) Titration of SMRT with TLX confirmed a TLX-SMRT interaction. Data are the mean±SD; N=3. (e) The TLX-SMRT interaction was responsive to istradefylline (**30**) but not ccrp2. Data are the mean±SD; N=3. (f) Istradefylline (**30**) and ccrp2 promoted TLX-RXR heterodimerization, **8** and **29** had no pronounced effect. All compounds were used at 10 μM Data are the mean±SD; N=3. (g) In cellular setting, Gal4-TLX recruited a VP16-RXRα-LBD fusion protein as observed by a dose-dependent increase in reporter activity. Data are mean±S.E.M. relative light units (RLU); n=3. (h) The TLX-RXR interaction was responsive to istradefylline (**30**) also in the cellular setting. Data are mean±S.E.M. relative reporter activity vs. DMSO; n=6. *** p<0.001 (t-test vs. DMSO).

To elucidate the mechanism by which ligands modulate TLX activity, we probed the response of the TLX LBD on ligand binding in various homogenous time-resolved fluorescence resonance energy transfer (HTRF)-based settings using Tb^{3+}-cryptate or sGFP-labeled nuclear receptor ligand binding domains and Tb^{3+}-cryptate or fluorescein-labeled co-regulator peptides. An association of the TLX LBD with atrophin has been described previously prompting us to determine ligand effects on the affinity between TLX and the Atro box peptide[20]. The TLX LBD robustly and specifically recruited the Atro box peptide[20], an interaction incompetent mutant[21] was not bound (Figure 3a).

The TLX-atrobox interaction was, however, not modulated by caffeine (**8**), **29**, istradefylline (**30**) or the previously reported TLX ligand ccrp2 (Figure 3b). We hypothesized that other nuclear receptor co-regulators might involve in TLX regulation and the receptor's response to ligands. Thus, we screened twenty-nine canonical co-regulator interaction motifs for recruitment to TLX in apo-state or in presence of varying concentrations of caffeine (**8**, Figure S6). High HTRF indicated potential binding of nuclear receptor co-repressor 1 (NCoR1) and silencing mediator for retinoid or thyroid-hormone receptors (SMRT, also termed NCoR2) to the TLX LBD. Titration of NCoR1 and SMRT with the TLX LBD confirmed this assumption indicating similar or even higher affinity compared to the Atro box peptide (Figure 3c and d). The TLX-NCoR1 interaction showed no response to TLX modulators **8**, **29**, **30** or ccrp2 (Figure 3c), however, the interaction of TLX with the repressor SMRT was markedly decreased by istradefylline (**30**, Figure 3e) aligning with the inverse TLX agonism we observed in the VP16/TLX assay. These results suggest that TLX modulation by xanthines is at least in part mediated through the TLX-SMRT interaction. Still, additional mechanisms might involve in TLX modulation by ligands, and we hypothesized heterodimerization of TLX as potential further mediator of ligand effects in line with the repressor activity of TLX. When we titrated Tb^{3+}-cryptate-labeled TLX LBD with sGFP-labeled RXRα LBD in presence of TLX ligands, we observed indeed enhanced dimerization for istradefylline (**30**) and ccrp2 while caffeine (**8**) and **29** had only weak effects (Figure 3f).

Following up on our observation that the recombinant LBDs of TLX and RXRα dimerized (Figure S1d) and that this interaction was responsive to **30** (Figure 3f), we further probed whether TLX and RXR would also interact in cellular setting. For this, we co-transfected HEK293T cells with Gal4-responsive firefly luciferase, constitutive renilla luciferase, and a VP16-RXRα-LBD fusion construct with or without Gal4-TLX (Figure 3g). In absence of Gal4-TLX, VP16-RXRα failed to induce reporter transcription but upon addition Gal4-TLX, reporter activity increased with increasing Gal4-TLX doses demonstrating that the interaction between the TLX and RXRα LBDs is relevant in cells as well. When we studied the effect of istradefylline (**30**) on this interaction (Figure 3h), we detected an increase in the TLX-RXRα interaction as observed in elevated reporter activity. These findings support our observation of a TLX repressor activity on various nuclear receptors and further suggest that direct LBD interactions are involved in these effects.

To further characterize the effects of xanthines on TLX activity and evaluate TLX modulation in a native cellular setting, we treated human glioblastoma cells (T98G) with caffeine (**8**), **29**, istradefylline (**30**), or **33**, and determined changes in TLX regulated gene expression by quantitative real-time PCR (Figure 4). All four studied xanthines **8**, **29**, **30** and **33** enhanced expression of the NAD-dependent deacetylase sirtuin-1 (SIRT1, Figure 4a), the cyclin-dependent kinase inhibitor 1 (p21, Figure 4b), and the solute carrier family 1 member 1 (SLC1a1, Figure 4c),

all of which are known as TLX regulated[16,22–27]. Importantly, the expression of TLX (Figure 4d) was not affected further indicating that the xanthines affect TLX regulated gene expression through direct TLX modulation.
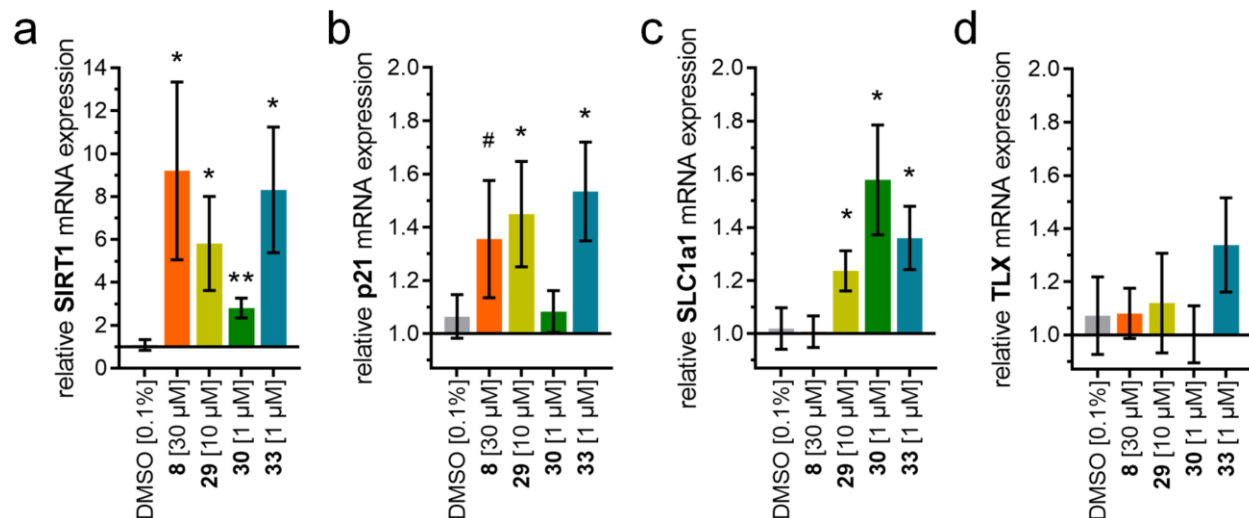
Figure 4. Effects of xanthines on TLX regulated gene expression in human T98G glioblastoma cells. The xanthines **8**, **29**, **30** and **33** enhanced expression of the TLX regulated genes SIRT1 (a), p21 (b) and SLC1a1 (c). Expression of TLX (d) was not affected. Data are mean±S.E.M. relative mRNA expression; n=8. # $p<0.1$, * $p<0.05$, ** $p<0.01$ (t-test vs DMSO).

The orphan NR TLX – exclusively expressed in certain areas of the CNS – increasingly attracts attention for its potential as therapeutic target in neurodegenerative and neurological disorders or for brain tumors. However, studies on TLX biology beyond knockout experiments are hindered by the lack of potent and well-characterized TLX modulators to be employed as tool compounds for functional experiments. Moreover, the molecular mode of TLX activity and its modulation by small molecule ligands remain widely elusive complicating the search for TLX ligands and early drug discovery. To overcome these obstacles in TLX target validation, we have designed a screening system for TLX ligands, screened for TLX modulators and employed these as tools for early functional studies.

As a key in vitro tool, we constructed a robust cellular assay system to mimic the repressor role of TLX by combining the transcriptional repressor Gal4-TLX with the potent ligand-independent transcriptional activator Gal4-VP16. An ability of Gal4-TLX to counter Gal4-VP16 induced reporter gene activity in a dose-dependent fashion allowed tuning of the test setup to observe bidirectional TLX modulation. Despite its artificial character, this cellular test system turned out very valuable for the discovery and preliminary characterization of TLX ligands, and might also be transferable to other repressive nuclear receptors such as the testicular receptors (TR). Importantly, our observations on Gal4-VP16 repression by Gal4-TLX also translated to combinations of TLX with

human NRs. This validated the TLX/VP16 setting, but also unprecedentedly revealed TLX acting as a repressor towards various nuclear receptors and dimerization of TLX with RXR in cell-free setting additionally demonstrated direct interaction.

In the VP16/TLX assay, caffeine directly modulated TLX and counteracted its repressor activity with an IC_{50} value of 9 µM. We also observed an ability of caffeine to reverse TLX-mediated repression of various NRs. Considering that typical caffeine concentrations after coffee consumption or pharmacological caffeine intake peak at 10 mg/L (~ 50 µM)[28] plasma levels and that brain penetration of caffeine is high[28], this unprecedented molecular activity of caffeine has potential biological relevance. Importantly, habitual caffeine intake has been correlated with reduced risk for Parkinson's Disease[29–31] and Alzheimer's Disease[32,33]. As TLX is an essential factor of neural maintenance and neurogenesis[16,27], a potential connection of these effects is obvious.

Systematic structural modification of the caffeine chemotype favourably led to a dramatic increase in potency on TLX, exemplified by **29** (IC_{50} 160 nM, 2.9-fold TLX repression), **33** (40 nM, 4.0-fold) and **34** (9 nM, 3.0-fold). In addition, we discovered the recently approved drug istradefylline (**30**) as a potent TLX modulator (IC_{50} 40 nM, 2.6-fold TLX repression). This activity might prove as important feature of the drug's pharmacological profile since TLX, characterized as essential regulator of NSC homeostasis and neurogenesis[3,7,27], could involve in the pathology and treatment of PD. Furthermore, TLX is a crucial factor for spatial learning[6–8] and a recent rodent AD model has demonstrated improvements in memory and spatial learning in istradefylline treated animals[34] further suggesting a potential involvement of TLX in the drug's pharmacology.

Our mutagenesis study suggested residues in the core region of the TLX LBD involved in TLX modulation by xanthines. In essence, we found Phe226 and Ile230 located in helix 5 playing a role in mediating the effects of the xanthines. Moreover, consistent with previous studies[20] we observed recruitment of the Atro box peptide to the TLX LBD, yet this interaction was not altered by available ligands. From a large collection of canonical nuclear receptor co-regulators we screened, NCoR1 and SMRT emerged as further interaction partners of TLX of which the TLX-SMRT recruitment revealed robust modulation by istradefylline. In addition, we detected effects of TLX ligands on the dimerization of the LBDs of TLX and RXR, which might involve in TLX modulation by small molecule ligands. Importantly, the TLX-RXR interaction was observed in a cell-free HTRF-based test system and in an orthogonal cellular reporter gene assay. From these observations we conclude that TLX modulation by xanthines likely results from several contributing effects on protein interactions involving heterodimerization and co-regulator binding. With only a limited collection of potential interactors tested, we also hypothesize that further factors participate in this network.

Overall, we report a new biological activity of xanthines on the transcription factor TLX and add a new chemotype to the sparse collection of known TLX ligands. The xanthines emerge as tools for functional studies on TLX and as a valuable TLX ligand scaffold for medicinal chemistry. Modification of the xanthine scaffold in 8-position especially with small heterocycles was highly favored for TLX modulation. Additionally, our SAR elucidation suggests that further optimization potential may rest in the alkylation pattern in 1- and 3-positions of the xanthine. While we observed favorable selectivity of xanthines within the nuclear receptor family, future studies will also have to address specificity.

We demonstrate TLX modulation by xanthines in multiple orthogonal assays. Initially, we discovered TLX modulation by xanthines in a hybrid reporter gene assay built on Gal4-VP16 as transcriptional inducer to enable unfolding of Gal4-TLX's transcriptional repressor activity. In the VP16/TLX assay, xanthines counteracted the intrinsic activity of TLX as transcriptional repressor suggesting inverse agonism. Importantly, these effects of xanthines on reporter activity vanished when Gal4-VP16 but not Gal4-TLX were present which provided initial evidence for direct TLX mediated activity. It should be noted that the hybrid assay is highly artificial and does not reflect physiological settings but turned out very suitable for primary screening. The fact that TLX modulation by xanthines was confirmed in multiple further biochemical, biophysical, and cellular systems demonstrates that the VP16/TLX assay despite its artificial character is predictive of cellular TLX modulation. The xanthines were found to modulate TLX activity also in several other reporter gene assay settings and in native human glioblastoma cells in which we observed robust induction of TLX regulated genes without alterations in TLX expression. Enhanced p21 and SLC1a1 expression upon xanthine treatment suggests inhibition of TLX activity since TLX knockdown has been reported to upregulate expression of both genes, too[14,24]. Upregulation of SIRT1, in contrast, according to current understanding[22,23] indicates TLX activation by xanthines. These opposing modulatory effects on TLX activity might potentially suggest different mechanisms in TLX-mediated regulation of p21, SLC1a1 and SIRT1 expression.

While our data, hence, demonstrate direct modulation of the TLX LBD by xanthines, the molecular mechanism of this TLX activity will require future attention to confirm the ligand binding site and capture stabilizing or destabilizing effects of ligand binding that contribute to the modulation of TLX activity. We hypothesize that several molecular factors, including but likely not limited to heterodimerization with RXR and SMRT interactions, involve in the regulation of cellular TLX activity by xanthines. The higher potency we have observed for istradefylline in modulating TLX in cells compared to cell-free assays may hence be explained by the sum of several weaker contributions that cooperate in cellular environment. Further elucidation of this coregulatory

network of TLX and its response to ligand binding is needed for which the xanthines present as useful tool.

Conclusions

In summary, we characterize the natural product caffeine and the structurally related drug istradefylline as modulators of the orphan NR TLX. Both molecules exhibit biological effects in neurodegenerative diseases that correlate with the involvement of TLX in neural homeostasis and cognitive function pointing to a potential connection between TLX and the established biological effects of caffeine and istradefylline. The structurally optimized caffeine analogues **29**, **33** and **34** as well as istradefylline provide high potency on TLX with pronounced selectivity within the NR family and qualify as initial tool compounds for elucidating molecular function and biology of this understudied NR.

Experimental

Reporter gene assays

Plasmid constructs. pFR-Luc was used as a reporter plasmid (Stratagene, San Diego, CA, U.S.A). pRL-SV40 (Promega, Fitchburg, WI, U.S.A) served for normalization of cell growth and transfection efficiency, and to observe test compound toxicity. pECE-SV40-Gal4-VP16 was a gift from Lea Sistonen (Addgene plasmid # 71728; http://n2t.net/addgene:71728; RRID:Addgene_71728; Addgene, Watertown, MA, U.S.A) and was used as transcriptional inducer of reporter gene expression. Gal4 hybrid clones of human NRs were obtained by inserting the respective protein sequence including hinge region into pFA-CMV (Agilent Technologies). The Gal4-DBD fusion plasmid with TLX (NR2E1; uniprot entry: Q9Y466-1; residues 150-385) was constructed by integrating a cDNA fragment obtained from PCR amplification using the natural cDNA (TLX BC028031.1, purchased as I.M.A.G.E. cDNA clone #5242079 from Source BioScience, Nottingham, UK) as template between the BamHI cleavage site of pFA-CMV vector (Stratagene, La Jolla, CA, USA) and an afore inserted KpnI cleavage site. Variants with mutated TLX LBD were generated by site directed mutagenesis using Q5 high fidelity polymerase (New England Biolabs). The respective codons were changed according to optimal codon usage in human cells. All plasmids were verified by sequencing of the entire Gal4-TLX open reading frame. Generation of pFA-CMV-hCAR-LBD[35], pFA-CMV-hFXR-LBD[36], pFA-CMV-hLXRα-LBD[36], pFA-CMV-hLXRβ-LBD[36], pFA-CMV-hPPARα-LBD[37], pFA-CMV-hPPARγ-LBD[37], pFA-CMV-hPPARδ-LBD[37], pFA-CMV-hRARα-LBD[35], pFA-CMV-hRARβ-LBD[35], pFA-CMV-hRARγ-LBD[35], pFA-CMV-hRXRα-LBD[35], pFA-CMV-hRXRβ-LBD[35], pFA-CMV-hRXRγ-LBD[35], pFA-CMV-hVDR-LBD[35], pFA-CMV-hNur77-LBD[38], pFA-CMV-hNurr1-LBD[38] and pFA-CMV-hNOR1-LBD[38] has been described

previously. To study LBD heterodimer formation of TLX and RXRα in cellular context, an RXRα construct was needed which itself does not bind the Gal4 response element but is capable of recruiting the transcription machinery. In the original plasmid pFA-CMV the section encoding the Gal4-DBD (that starts with the eighth codon of the CMV controlled ORF) was replaced by a DNA sequence coding for VP16 (α trans inducing factor; uniprot P06492; aa 413-490) followed by a Gly-Ser linker. The resulting plasmid was termed pFTI-CMV (fusion trans-inducing factor plasmid). Into this plasmid the native cDNA sequence for human RXRα (aa 225-462) was inserted by gibson assembly between the restriction sites for BamHI and XbaI within the original multiple cloning site resulting in pFTI-CMV-VP16-RXRα-LBD. Expression of the fusion protein MDYKDDVAST-[VP16 (aa 413-490)]-SSGGGGSSGGS-[RXRα LBD (aa 225-262)] is under the control of the CMV promoter.

Gal4-TLX/Gal4-VP16 assay procedure. HEK293T cells were grown in Dulbecco´s modified Eagle´s medium (DMEM, ThermoFisher Scientific), high glucose with 10% fetal calf serum (FCS), sodium pyruvate (1 mM), penicillin (100 U/mL) and streptomycin (100 µg/mL) at 37 °C and 5% CO_2. 24 hours before transfection, cells were seeded in 96-well plates (30,000 cells/well) in DMEM with above mentioned supplements. Prior to transfection, medium was changed to Opti-MEM (ThermoFisher Scientific) without supplements. Cells were then transiently transfected with plasmid mixtures containing 100 ng/well pFR-Luc, 1 ng/well pRL-SV40, 6 ng/well of pECE-SV40-Gal4-VP16 and 3 ng/well of pFA-CMV-Gal4-TLX (during assay establishment, these plasmid amounts per well were systematically varied to optimize conditions allowing robust observation of bidirectional TLX modulation). Transient transfection was achieved using Lipofectamine LTX reagent (ThermoFisher Scientific) according to the manufacturer´s protocol. Five hours after transfection cells were treated with Opti-MEM supplemented with penicillin (100 U/mL) and streptomycin (100 µg/mL) additionally containing 0.1% dimethylsulfoxide (DMSO) and the respective test compounds or 0.1% DMSO alone as negative control. Each sample was tested in duplicates and every experiment was conducted at least three times. After 14 h incubation, cells were lysed for luciferase luminescence detection using the Dual-Glo Luciferase Assay System (Promega) according to the manufacturer´s protocol. Luminescence was measured with an Tecan Spark luminometer (Tecan Deutschland GmbH). To consider transfection efficiency and cell growth, the obtained firefly luciferase signal was normalized by dividing firefly luciferase signals by renilla luciferase signals and multiplying by a factor of 1000 to obtain relative light units (RLU). Fold reporter activation or repression was obtained by dividing the mean RLU of a test compound at a respective concentration by the mean RLU of the 0.1% DMSO control. IC_{50} values were obtained by plotting fold reporter activation vs test compound concentrations and fitting the resulting sigmoidal curve with a four parameter logistic regression in SigmaPlot 12.5. Separate

control experiments were performed following the same procedure with the exception that cells were only transfected with 100 ng/well pFR-Luc, 1 ng/well pRL-SV40 and 6 ng/well pECE-SV40-Gal4-VP16 to exclude unspecific cellular or VP16 mediated effects. Experiments with the TLX mutants were performed equally using the respective mutant clones pFA-CMV-Gal4-TLX$_{A189E}$, pFA-CMV-Gal4-TLX$_{L268R}$, pFA-CMV-Gal4-TLX$_{A189E/L268R}$, pFA-CMV-Gal4-TLX$_{F226W/I230E}$ or pFA-CMV-Gal4-TLX$_{A189E/F226W/I230E}$ instead of wild-type pFA-CMV-Gal4-TLX.

Gal4-TLX/Gal4-NR assay procedures. Interaction of Gal4-TLX with diverse human NRs in Gal4-format was studied in identical procedures to the Gal4-TLX/Gal4-VP16 experiments with varying concentrations of pFA-CMV-Gal4-TLX (0, 0.5, 1, 3, 6, 12 ng/well) and the respective Gal4-NR clones (fixed concentration). Amounts of reporter (pFR-Luc, 100 ng/well) and control (pRL-SV40, 2 ng/well) were fixed. NRs with low intrinsic activity were activated by using reference agonists at 1 µM. Plasmid amounts and reference agonists were as follows: Gal4-CAR (25 ng/well, CITCO); Gal4-FXR (25 ng/well, GW4064), Gal4-LXRα (50 ng/well, T0901317), Gal4-LXRβ (50 ng/well, T0901317), Gal4-Nurr1 (6 ng/well), Gal4-PPARα (25 ng/well, GW7647), Gal4-PPARγ (25 ng/well, pioglitazon), Gal4-PPARδ (25 ng/well, L165041), Gal4-RARα (12 ng/well, tretinoin), Gal4-RARβ (12 ng/well, tretinoin), Gal4-RARγ (12 ng/well, tretinoin), Gal4-RORα (6 ng/well), Gal4-RXRα (12 ng/well, bexarotene), Gal4-RXRβ (12 ng/well, bexarotene), Gal4-RXRγ (12 ng/well, bexarotene) and Gal4-VDR (25 ng/well, calcitriol).

Gal4-TLX/VP16-RXRα assay procedure. Interaction of Gal4-TLX with VP16-RXRα was studied according to the Gal4-TLX/Gal4-VP16 experimental procedure with co-transfection of varying amounts of pFTI-CMV-VP16-RXRα (0, 0.5, 1, 3, 6 ng/well). 3 or 12 ng/well Gal4-TLX, 100 ng/well pFR-Luc and 1 ng/well pRL-SV40 were used.

Quantification of TLX and TLX-regulated gene expression in human glioblastoma cells

T98G cells (European Collection of Authenticated Cell Cultures) were cultured in Dulbecco´s modified Eagle´s medium (DMEM, ThermoFisher Scientific), high glucose supplemented with 10% fetal calf serum (FCS), sodium pyruvate (1 mM), penicillin (100 U/mL) and streptomycin (100 µg/mL) at 37 °C and 5% CO_2. For the experiments, cells were seeded in 6-well plates (1 x 10^6 cells/well). After 24 h, medium was changed to Minimal Essential Medium (MEM) supplemented with 1% charcoal-stripped FCS, penicillin (100 U/mL), streptomycin (100 µg/mL) and 2 mM L-glutamine. 24 h later T98G were incubated with the test compounds (caffeine (**8**, 30 µM), **29** (10 µM), istradefylline (**30**, 1 µM), and **33** (1 µM)) dissolved in the same medium additionally containing 0.1 % DMSO or with 0.1 % DMSO as untreated control for 8 h. Cells were then harvested, washed with phosphate-buffered saline (PBS) and used directly for mRNA extraction by the E.Z.N.A.® Total RNA Kit I (R6834-02, Omega Bio-Tek, Inc., Norcross, GA, USA). Extracted mRNA was

reverse transcribed into cDNA using High-Capacity RNA-to-cDNA™ Kit (4387406, Thermo Fischer Scientific, Inc.). TLX target gene expression was analysed by quantitative real-time PCR (qRT-PCR) with a StepOnePlus System (Life Technologies, Carlsbad, CA, USA) using Power SYBR® Green (Life Technologies). Each sample was analysed in duplicates and repeated in at least eight independent experiments. Data were analysed by the comparative ΔΔCT method with glyceraldehyde 3-phosphate dehydrogenase (GAPDH) as reference gene. The following primers were used for T98G cells (human genes): GAPDH[39]: forward 5' - CCT GTT CGA CAG TCA GCC G - 3', reverse 5' – CGA CCA AAT CCG TTG ACT CC - 3' p21 (Origene, Rockville, MD, U.S.A.): forward 5' - AGG TGG ACC TGG AGA CTC TCA G - 3', reverse 5' - TCC TCT TGG AGA AGA TCA GCC G - 3'; SIRT1[22]: forward 5' - GAA CCT TTG CCT CAT CTA CA - 3', reverse 5' - AGC CGC TTA CTA ATC TGC TC - 3'; SLC1a1[14]: forward 5` - CGA AAG AAC CCT TTC CGA TTT GC - 3', reverse 5' - GAA GGT GAC AGG CAG TGT TGC T - 3'; TLX: forward 5' – CTA AGA GTG TGC CAG CCT TC - 3', reverse 5' – TGT TAG CAT CAA CCG GAA TGG - 3'.

Protein expression

TLX protein expression. Recombinant TLX LBD with an N-terminal His_6-tag was expressed in *E.coli* Rosetta*.* Cells were initially cultured in TB medium at 37 °C to an OD_{600} of 2.8 prior to induction with 0.5 mM IPTG at 18°C overnight. Cells were harvested and resuspended in a buffer containing 50 mM HEPES pH 7.5, 500 mM NaCl, 20 mM imidazole, 5% glycerol and 1 mM TCEP. Recombinant TLX LBD was initially purified by Ni^{2+} affinity chromatography. The histidine tag was removed by TEV protease treatment, and the cleaved protein was separated by reverse Ni^{2+} affinity purification. The protein was further purified by size exclusion chromatography and stored in 20 mM Tris, pH 7.5, 150 mM NaCl, 0.2 mM TCEP and 5% glycerol.

Expression and purification of recombinant RXRα and TLX fusion proteins. The coding sequence for RXRα LBD (uniprot entry: P19793-1, residues 226-462) and TLX LBD (uniprot entry: Q9Y466-1, residues 150-385) was codon optimized for *E.coli* and purchased from Geneart (Regensburg, Germany)*,* respectively. For expression of the RXRα fusion protein with N-terminal green fluorescent protein (GFP), an expression construct based on pET29b was prepared. For this, the entire section between the original NdeI site and the fourth position following the His-Tag coding sequence of pET29b was replaced, hence, essentially leaving only the vector backbone unmodified. The section was replaced by a sequence encoding a restriction site for NcoI (overlapping with the start codon) and an open reading frame for Met-Gly-[His_{10}-Tag]-Asp-Tyr-Asp-Ile-Pro-Thr-Thr-[TEV site]-superfolder GFP[40] followed by restriction sites for BamHI (in frame) and XhoI. The sequence coding for the RXRα LBD followed by a stop codon was then introduced in frame between the afore inserted restriction site for BamHI and XhoI. For expression of TLX

17

LBD with N-terminal GFP the sequence encoding TLX residues 150-385 was cloned between the same sites. For generation of biotinylated TLX LBD, the pMal vector system (New England Biolabs, NEB, Ipswich, MA, USA) was used. In pMal-c2E, the section between the sequence encoding 10x Asparagine (Asn_{10}) and the SalI restriction site was replaced with a sequence encoding Leu-Gly-Ile-Glu-Leu-Val-[His_8-Tag]-Asp-Tyr-Asp-Ile-Pro-Gly-Thr-Leu-[TEV site] followed by an Avi-Tag and restriction sites for BamHI and XhoI. The sequence encoding TLX followed by two stop codons was cloned in frame between these restriction sites. From this construct, a fusion protein is expressed with N-terminal maltose-binding protein (MBP) followed by an Asn_{10} linker, a His_8-Tag, a cleavage site for TEV protease, an Avi-Tag, and the TLX LBD with unmodified C-terminus. For expression, E. coli T7 express cells (NEB) were co-transformed with pGro7 (TAKARA Bio Inc., Kusatsu, Japan) and the aforementioned expression construct, and selected overnight at 37°C on LB (Luria Broth) agar containing 34 µg/ml chloramphenicol and either 100 µg/ml ampicillin (for pMal) or 35 µg/ml kanamycin (for pET). Culture in liquid LB was inoculated and grown at 37°C with constant shaking at 180 rpm until optical density at 600 nm (OD_{600}) reached 0.7. At this time point, expression of the chaperone GroEL/ES from pGro7 was induced with 1 g/L L(+)-arabinose and the temperature was reduced to 20°C. At OD_{600} = 1, expression of the target protein was induced by addition of 0.5 mM IPTG. After 12-16 h, cells were harvested by centrifugation and resuspended in buffer A (400 mM NaCl, 20 mM NaP_i pH 7,8, 10% (w/v) glycerol and 20 mM ß-mercaptoethanol). Cells were kept on ice and disrupted in presence of 1 mM ATP, DNAse I, RNAse A, 20 mM $MgSO_4$, and EDTA-free cOmplete™ protease inhibitor cocktail (F. Hoffmann-La Roche AG, Basel, Switzerland) by addition of lysozyme and 10 passages through an Invensys APV-1000 homogenizer (APV Systems, Silkeborg, Denmark). Cell debris was removed by centrifugation at 16500 x g for 20 minutes at 4°C.

Purification was achieved by immobilized metal affinity chromatography (IMAC) using columns packed with Ni Sepharose 6 Fast Flow resin on an ÄKTApurifier FPLC system (GE Healthcare, Chicago, IL, USA). After washing with buffer supplemented with 50 mM imidazole, the protein was eluted with 300 mM imidazole. Afterwards, GFP fusion proteins were processed with His tagged TEV protease overnight while imidazole content was reduced to 10 mM by dialysis against buffer A in order to allow for reverse IMAC. The flow through was concentrated and applied to size exclusion chromatography using a 16/60 Superdex200™ column equilibrated and run in HTRF assay buffer [25 mM HEPES pH 7.5, 150 mM KF, 10% (w/v) glycerol, 5 mM DTT]. Following the initial IMAC purification step, the MBP fusion protein for generation of biotin labeled TLX LBD was processed with MBP-tagged TEV protease during overnight dialysis against buffer A. Afterwards, uncleaved fusion protein, free MBP-Tag, and TEV protease were removed by passaging through a gravity flow column packed with Amylose High Flow resin (NEB). The flow through was then

supplemented with 0.5 mM biotin, 0.5 mM ATP, 5 mM MgCl$_2$, and E. coli biotin ligase birA at a molar ratio of approx. 1:10 for enzymatic conjugation of biotin to the lysine residue in the avitag. After overnight incubation at 4°C, the solution was subjected to a column packed with 5 ml monomeric avidin UltraLink™ resin (Pierce Biotechnology Inc., Rockford, IL, USA). Unlabeled protein and birA were removed by washing for 10 column volumes with buffer A before biotin labeled TLX LBD was eluted using buffer A supplemented with 2 mM biotin. The product was then concentrated and subjected to size exclusion chromatography using a 10/30 Superdex75™ column equilibrated and run in HTRF assay buffer.

NMR spectroscopy

Spectra acquisition was carried out on a Bruker 600MHz AVIIIHD spectrometer equipped with a 5 mm a nitrogen-cooled triple resonance probe ^{1}H/^{19}F [^{13}C,^{15}N]-TCI (Prodigy) and high throughput sample changer (SampleJet) for 579 samples with temperature option for sample storage. All spectra were acquired and processed using Bruker software Topspin 3.6.2 and Topspin 4.0.9, respectively. For the TLX-ligand interaction studies, two samples (with and without protein) were prepared. ^{1}H-1D, water-suppressed proton 1D (zgesgppe[41], water suppression using excitation sculpting with gradients using perfect echo) was acquired for each of the sample. Interaction studies were performed at a ratio of 1:1 with respect to TLX and the ligand. The final [protein]-ligand concentration was 50 µM. A sample volume of 200 µl in the buffer (20 mM Tris pH 7.5; 150 mM NaCl; 0.2 mM TCEP) with 5% D$_2$O (NMR lock solvent) and 100 µM of TMSP-Na as NMR internal reference (Chemical shift reference) was prepared and transferred to a 3 mm NMR-tube for measurement. The samples were stored at 4 °C and measured at 298 K.

HTRF assays

Co-regulator preference screen. Recruitment of co-regulator peptides to recombinant TLX-LBD was studied in a homogeneous time-resolved fluorescence resonance energy transfer (HT-FRET) assay system. Terbium cryptate as streptavidin conjugate (Tb-SA; Cisbio assays, France) was coupled to biotinylated recombinant TLX-LBD protein and served as FRET donor. Fluorescein-labeled co-regulator peptides as FRET acceptors were purchased (ThermoFisher Scientific). Assay solutions were prepared in HEPES buffer [25 mM HEPES pH 7.5, 150 mM KF, 10% (w/v) glycerol, 5 mM DTT, 0.1% (w/v) CHAPS] and contained recombinant biotinylated TLX-LBD (3 nM), Tb-SA (3 nM) and the respective fluorescein-labeled co-regulator peptide (100 nM) as well as 1% DMSO and **8** (1, 10 or 100 µM) or DMSO alone as negative control. After 2 h incubation at RT, fluorescence intensities (FI) after excitation at 340 nm were recorded at 520 nm for fluorescein acceptor fluorescence and 620 nm for Tb-SA donor fluorescence on Tecan SPARK luminometer

(Tecan Group Ltd.). FI520nm was divided by FI620nm and multiplied with 10,000 to give a dimensionless HTRF signal.

Co-regulator affinity assay. Strength and modulation of affinity for individual co-regulators was investigated by titration of GFP-TLX LBD against FRET donor coupled co-regulator peptide. Assay solutions were prepared in HTRF assay buffer supplemented with 0.1% (w/v) CHAPS as well as 1% DMSO with test compounds at 10 µM or DMSO alone as negative control. The FRET donor complex formed from biotinylated co-regulator peptide wild type Atrobox peptide (biotin-PPYADTPALRQLSEYARPHVAFSP); recruitment deficient mutant Atrobox peptide (biotin-PPYADTPAARQASEYARPHVAFSP); NCOR1 (ID2) (biotin-GHSFADPASNLGLEDIIRKALMGSFD); SMRT (ID2) (biotin-SQAVQEHASTNMGLEAIIRKALMGKYDQW) coupled to Tb-SA (12 nM) was kept constant while the concentration of GFP-TLX LBD was varied starting with 4 µM as the highest concentration. Free GFP was added to keep the total GFP content stable at 4 µM throughout the entire series in order to suppress artefacts from changes in degree of diffusion enhanced FRET. After 1 h incubation at RT, fluorescence intensities (FI) after excitation at 340 nm were recorded at 520 nm for GFP acceptor fluorescence and 620 nm for Tb-SA donor fluorescence on a SPARK plate reader (Tecan Group Ltd.). FI520nm was divided by FI620nm and multiplied with 10,000 to give a dimensionless HTRF signal. Modulation of recruitment of SMRT by increasing concentrations of ccrp2 and Istradefyllin was assayed with a constant concentration of 100 nM (ccrp2) or 200 nM (Istradefyllin) GFP-TLX LBD.

TLX:RXR heterodimerization. Strength and modulation of the formation of the heterodimer composed of the LBDs of TLX and RXRα was investigated by titration of GFP-RXRα LBD against a fixed concentration of TLX LBD. Assay solutions were prepared in HTRF assay buffer supplemented with 0.1% (w/v) CHAPS as well as 1% DMSO with test compounds at 100 µM or DMSO alone as negative control. The FRET donor complex formed from biotinylated TLX LBD (final concentration 0.375 nM) and Tb-SA (0.75 nM) was kept constant while the concentration of GFP-RXRα LBD was varied starting with 600 nM as the highest concentration. Total GFP was again kept constant throughout the entire experiment by supplementation with free GFP, and measurement was performed as described before for the co-regulator affinity assay.

For further experimental details, please refer to the Supporting Information.

Conflicts of interest

There are no conflicts to declare.

Acknowledgements

References

1. Shi, Y. *et al.* Expression and function of orphan nuclear receptor TLX in adult neural stem cells. *Nature* **427**, 78–83 (2004).

2. Miyawaki, T. Tlx, an Orphan Nuclear Receptor, Regulates Cell Numbers and Astrocyte Development in the Developing Retina. *J. Neurosci.* **24**, 8124–8134 (2004).

3. Liu, H. K. *et al.* The nuclear receptor tailless is required for neurogenesis in the adult subventricular zone. *Genes Dev.* **22**, 2473–2478 (2008).

4. Abrahams, B. S. Pathological Aggression in 'Fierce' Mice Corrected by Human Nuclear Receptor 2E1. *J. Neurosci.* **25**, 6263–6270 (2005).

5. Davis, S. M., Thomas, A. L., Nomie, K. J., Huang, L. & Dierick, H. A. Tailless and atrophin control drosophila aggression by regulating neuropeptide signalling in the pars intercerebralis. *Nat. Commun.* **5**, 1–10 (2014).

6. O'Leary, J. D. *et al.* The nuclear receptor Tlx regulates motor, cognitive and anxiety-related behaviours during adolescence and adulthood. *Behav. Brain Res.* **306**, 36–47 (2016).

7. Kozareva, D. A., O'Leary, O. F., Cryan, J. F. & Nolan, Y. M. Deletion of TLX and social isolation impairs exercise-induced neurogenesis in the adolescent hippocampus. *Hippocampus* **28**, 3–11 (2018).

8. O'Leary, J. D., O'Leary, O. F., Cryan, J. F. & Nolan, Y. M. Regulation of behaviour by the nuclear receptor TLX. *Genes, Brain Behav.* **17**, 1–11 (2018).

9. Kumar, R. A. *et al.* Initial association of NR2E1 with bipolar disorder and identification of candidate mutations in bipolar disorder, schizophrenia, and aggression through resequencing. *Am. J. Med. Genet. Part B Neuropsychiatr. Genet.* **147**, 880–889 (2008).

10. Zou, Y. *et al.* The Nuclear Receptor TLX Is Required for Gliomagenesis within the Adult

Neurogenic Niche. *Mol. Cell. Biol.* **32**, 4811–4820 (2012).

11. Chavali, P. L. *et al.* TLX activates MMP-2, promotes self-renewal of tumor spheres in neuroblastoma and correlates with poor patient survival. *Cell Death Dis.* **5**, e1502 (2014).

12. Benod, C. *et al.* The human orphan nuclear receptor tailless (TLX, NR2E1) is druggable. *PLoS One* **9**, e99440 (2014).

13. Cherkasov, A. Cherkasov_2018_computer aided discovery of small molecule inhibitors of transcriptional activity of TLX nuclear receptor.pdf. *Molecules* **23**, 1–10 (2018).

14. Griffett, K. *et al.* The Orphan Nuclear Receptor TLX Is a Receptor for Synthetic and Natural Retinoids. *Cell Chem. Biol.* **27**, 1272–1284 (2020).

15. Sadowski, I., Ma, J., Triezenberg, S. & Ptashne, M. GAL4-VP16 is an unusually potent transcriptional activator. *Nature* **335**, 563–564 (1988).

16. Sun, G., Yu, R. T., Evans, R. M. & Shi, Y. Orphan nuclear receptor TLX recruits histone deacetylases to repress transcription and regulate neural stem cell proliferation. *Proc. Natl. Acad. Sci. U. S. A.* **104**, 15282–7 (2007).

17. Yokoyama, A., Takezawa, S., Schule, R., Kitagawa, H. & Kato, S. Transrepressive Function of TLX Requires the Histone Demethylase LSD1. *Mol. Cell. Biol.* **28**, 3995–4003 (2008).

18. Zhang, C. L., Zou, Y., Yu, R. T., Gage, F. H. & Evans, R. M. Nuclear receptor TLX prevents retinal dystrophy and recruits the corepressor atrophin1. *Genes Dev.* **20**, 1308–1320 (2006).

19. Estruch, S. B. *et al.* The oncoprotein BCL11A binds to orphan nuclear receptor TLX and potentiates its transrepressive function. *PLoS One* **7**, 1–7 (2012).

20. Zhi, X. *et al.* Structural basis for corepressor assembly by the orphan nuclear receptor TLX. *Genes Dev.* **29**, 440–50 (2015).

21. Corso-Díaz, X. *et al.* Co-activator candidate interactions for orphan nuclear receptor NR2E1. *BMC Genomics* **17**, 832 (2016).

22. Iwahara, N., Hisahara, S., Hayashi, T. & Horio, Y. Transcriptional activation of NAD+-dependent protein deacetylase SIRT1 by nuclear receptor TLX. *Biochem. Biophys. Res. Commun.* **386**, 671–675 (2009).

23. Wu, D. *et al.* Orphan nuclear receptor TLX functions as a potent suppressor of oncogene-induced senescence in prostate cancer via its transcriptional co-regulation of the CDKN1A (p21$^{WAF1/CIP1}$) and SIRT1 genes. *J. Pathol.* **236**, 103–115 (2015).

24. O'Loghlen, A. *et al.* The nuclear receptor NR2E1/TLX controls senescence. *Oncogene* **34**, 4069–4077 (2015).

25. Monaghan, A. P. *et al.* Defective limbic system in mice lacking the tailless gene. *Nature*

390, 515–517 (1997).

26. Yu, R. T. *et al.* The orphan nuclear receptor Tlx regulates Pax2 and is essential for vision. *Proc. Natl. Acad. Sci.* **97**, 2621–2625 (2000).

27. Islam, M. M. & Zhang, C.-L. TLX: A master regulator for neural stem cell maintenance and neurogenesis. *Biochim. Biophys. Acta - Gene Regul. Mech.* **1849**, 210–216 (2015).

28. Nehlig, A. Interindividual Differences in Caffeine Metabolism and Factors Driving Caffeine Consumption. *Pharmacol. Rev.* **70**, 384–411 (2018).

29. Ascherio, A. *et al.* Prospective study of caffeine consumption and risk of Parkinson's disease in men and women. *Ann. Neurol.* **50**, 56–63 (2001).

30. Liu, R. *et al.* Caffeine Intake, Smoking, and Risk of Parkinson Disease in Men and Women. *Am. J. Epidemiol.* **175**, 1200–1207 (2012).

31. Hu, G., Bidel, S., Jousilahti, P., Antikainen, R. & Tuomilehto, J. Coffee and tea consumption and the risk of Parkinson's disease. *Mov. Disord.* **22**, 2242–2248 (2007).

32. Eskelinen, M. H., Ngandu, T., Tuomilehto, J., Soininen, H. & Kivipelto, M. Midlife Coffee and Tea Drinking and the Risk of Late-Life Dementia: A Population-Based CAIDE Study. *J. Alzheimer's Dis.* **16**, 85–91 (2009).

33. Maia, L. & de Mendonca, A. Does caffeine intake protect from Alzheimer's disease? *Eur. J. Neurol.* **9**, 377–382 (2002).

34. Orr, A. G. *et al.* Istradefylline reduces memory deficits in aging mice with amyloid pathology. *Neurobiol. Dis.* **110**, 29–36 (2018).

35. Flesch, D. *et al.* Non-acidic farnesoid X receptor modulators. *J. Med. Chem.* **60**, 7199–7205 (2017).

36. Heitel, P., Achenbach, J., Moser, D., Proschak, E. & Merk, D. DrugBank screening revealed alitretinoin and bexarotene as liver X receptor modulators. *Bioorg. Med. Chem. Lett.* **27**, 1193–1198 (2017).

37. Rau, O. *et al.* Carnosic acid and carnosol, phenolic diterpene compounds of the labiate herbs rosemary and sage, are activators of the human peroxisome proliferator-activated receptor gamma. *Planta Med.* **72**, 881–887 (2006).

38. Willems, S. *et al.* The orphan nuclear receptor Nurr1 is responsive to non-steroidal anti-inflammatory drugs. *Commun. Chem.* **3**, 85 (2020).

39. Schmidt, J. *et al.* NSAIDs Ibuprofen, Indometacin, and Diclofenac do not interact with Farnesoid X Receptor. *Sci. Rep.* **5**, 14782 (2015).

40. Pédelacq, J. D., Cabantous, S., Tran, T., Terwilliger, T. C. & Waldo, G. S. Engineering and characterization of a superfolder green fluorescent protein. *Nat. Biotechnol.* **24**, 79–88 (2006).

41. Adams, R. W., Holroyd, C. M., Aguilar, J. A., Nilsson, M. & Morris, G. A. "Perfecting" WATERGATE: Clean proton NMR spectra from aqueous solution. *Chem. Commun.* **49**, 358–360 (2013).